


Toll-like receptor 7/8 agonist R848 alters the immune tumor microenvironment and enhances SBRT-induced antitumor efficacy in murine models of pancreatic cancer

Jian Ye ^{1,2}, Bradley N Mills,^{1,3} Shuyang S Qin,^{1,4} Jesse Garrett-Larsen,^{1,2} Joseph D Murphy,^{1,4} Taylor P Uccello,^{1,4} Booyeon J Han,^{1,4} Tara G Vrooman,^{1,4} Carl J Johnston,^{3,5} Edith M Lord,^{2,3,4} Brian A Belt,^{1,2} David C Linehan,^{1,2,3} Scott A Gerber^{1,2,3,4}

To cite: Ye J, Mills BN, Qin SS, *et al.* Toll-like receptor 7/8 agonist R848 alters the immune tumor microenvironment and enhances SBRT-induced antitumor efficacy in murine models of pancreatic cancer. *Journal for ImmunoTherapy of Cancer* 2022;**10**:e004784. doi:10.1136/jitc-2022-004784

► Additional supplemental material is published online only. To view, please visit the journal online (<http://dx.doi.org/10.1136/jitc-2022-004784>).

Accepted 22 June 2022



© Author(s) (or their employer(s)) 2022. Re-use permitted under CC BY-NC. No commercial re-use. See rights and permissions. Published by BMJ.

For numbered affiliations see end of article.

Correspondence to

Dr Scott A Gerber;
scott_gerber@urmc.rochester.edu

ABSTRACT

Background Stereotactic body radiotherapy (SBRT) has been increasingly used as adjuvant therapy in pancreatic ductal adenocarcinoma (PDAC), and induces immunogenic cell death, which leads to the release of tumor antigen and damage-associated molecular patterns. However, this induction often fails to generate sufficient response to overcome pre-existing tumor microenvironment (TME) immunosuppression. Toll-like receptor (TLR) 7/8 ligands, such as R848, can amplify the effect of tumor vaccines, with recent evidence showing its antitumor effect in pancreatic cancer by modulating the immunosuppressive TME. Therefore, we hypothesized that the combination of R848 and SBRT would improve local and systemic antitumor immune responses by potentiating the antitumor effects of SBRT and reversing the immunosuppressive nature of the PDAC TME.

Methods Using murine models of orthotopic PDAC, we assessed the combination of intravenous TLR7/8 agonist R848 and local SBRT on tumor growth and immune response in primary pancreatic tumors. Additionally, we employed a hepatic metastatic model to investigate if the combination of SBRT targeting only the primary pancreatic tumor and systemic R848 is effective in controlling established liver metastases.

Results We demonstrated that intravenous administration of the TLR7/8 agonist R848, in combination with local SBRT, leads to superior tumor control compared with either treatment alone. The combination of R848 and SBRT results in significant immune activation of the pancreatic TME, including increased tumor antigen-specific CD8⁺ T cells, decreased regulatory T cells, and enhanced antigen-presenting cells maturation, as well as increased interferon gamma, granzyme B, and CCL5 along with decreased levels of interleukin 4 (IL-4), IL-6, and IL-10. Importantly, the combination of SBRT and systemic R848 also resulted in similar immunostimulatory changes in liver metastases, leading to improved metastatic control. CD8⁺ T cell depletion studies highlighted the necessity of these effector cells at both the local and hepatic metastatic sites. T cell receptor (TCR) clonotype analysis indicated that

WHAT IS ALREADY KNOWN ON THIS TOPIC

⇒ Toll-like receptor (TLR) 7/8 agonist R848 has been reported to modulate the immunosuppressive tumor microenvironment (TME) in pancreatic ductal adenocarcinoma (PDAC). However, whether the combination of radiotherapy and R848 improves tumor control and the antitumor immune response in local and metastatic PDAC models remains to be elucidated.

WHAT THIS STUDY ADDS

⇒ Systemic administration of R848 significantly augmented the stereotactic body radiotherapy (SBRT) induced antitumor response in mouse orthotopic and metastatic PDAC models. Mechanistically, SBRT induced immunogenic cell death locally at the site of irradiation releasing tumor antigens, while R848 amplified the vaccination effect by activating antigen-presenting cells and modulated the immunosuppressive TME in PDAC.

HOW THIS STUDY MIGHT AFFECT RESEARCH, PRACTICE OR POLICY

⇒ The combination of local SBRT and systemic R848 generated high-quality CD8⁺ T cells that infiltrated metastases providing a potential therapy for patients with both local and metastatic PDAC.

systemic R848 not only diversified the TCR repertoire but also conditioned the metastatic foci to facilitate entry of CD8⁺ T cells generated by SBRT therapy.

Conclusions These findings suggest that systemic administration of TLR7/8 agonists in combination with SBRT may be a promising avenue for metastatic PDAC treatment.

BACKGROUND

Pancreatic ductal adenocarcinoma (PDAC) is the most lethal cancer in the USA with a

5-year overall survival of only 9%, and cancer deaths associated with PDAC are expected to increase over the next 20 years.^{1,2} Due to the lack of early symptoms and rapid tumor progression, most patients present with locally advanced, unresectable, or metastatic disease where treatment options are limited.²

Radiotherapy is recommended for patients with PDAC with locally advanced tumors or borderline resectable tumors according to the guidelines of the National Comprehensive Cancer Network.³ Stereotactic body radiotherapy (SBRT) has largely replaced conventional radiotherapy during the past decade, emerging as a viable treatment modality for localized PDAC.^{4,5} SBRT enables precise delivery of high-dose radiation (20–35 Gy total) over a short period of time (5–6 fractions in 1–2 weeks), which is more convenient for patients and causes minimal radiation damage to surrounding tissues.^{6–8} Unfortunately, only a small percentage of patients with PDAC see clinical efficacy from SBRT, and these effects are modest and ultimately fall short of a durable response and meaningful survival benefit. This is largely the result of a unique PDAC tumor microenvironment (TME) that consists of a dense desmoplastic stroma with abundant immunosuppressive myeloid cells and few antitumor T cells.^{9–19} These characteristics dampen the efficacy of most PDAC therapies, including radiotherapy. Therefore, it is likely that SBRT would need to be combined with an immune-stimulating/repolarizing agent in order to achieve full antitumor potential in PDAC.

Immunogenic cell death (ICD) in tumors triggers the release of endogenous damage-associated molecular pattern molecules (DAMPs), which are essential to stimulate an optimal antitumor immune response.²⁰ Our previous work demonstrated that the magnitude of ICD and subsequent DAMP release following therapy-dictated treatment efficacy.²¹ This is largely attributed to intratumoral immune cells, such as dendritic cells (DCs), sensing the presence of these treatment-induced ‘danger’ signals by cellular receptors that ultimately stimulate adaptive immunity.²² Since our results demonstrate that more endogenous DAMPs result in heightened antitumor immunity, we investigated whether providing additional ‘danger’ signals exogenously (in the form of toll-like receptor (TLR) ligands) would artificially increase the magnitude of the cellular response to damage, and therapeutically enhance SBRT efficacy.

To accomplish this, we tested the TLR7/8 agonist, resiquimod (R848). TLR7 and TLR8 are commonly found on many cell types, including immune cells, and have been shown to induce the activation and maturation of DCs, along with reprogramming tumor-infiltrating macrophages and myeloid derived suppressor cells (MDSCs) from immunosuppressive to immunostimulatory.^{23,24} TLR7/8 are typically located in the endosomal compartments and sense the presence of ‘danger’ signals in the form of ssRNA.²⁴ Agonists such as FDA-approved imiquimod and the more potent resiquimod, which bind to TLR7/8 (TLR7 in the mouse and both

TLR7/8 in human) induce a potent immunostimulatory response.^{25,26} TLR7/8 agonists have been effective in amplifying the effects of tumor vaccines,^{25,27} and there is increasing evidence demonstrating that these particular agonists, when combined with standard of care therapies, may directly stimulate antitumor responses in various cancers. For example, preclinical studies using different tumor models, including lymphoma,²⁸ colorectal carcinoma, and fibrosarcoma²⁹ have demonstrated the generation of systemic antitumor immune responses following combination of radiotherapy and TLR7/8 agonist R848. There is recent evidence that TLR7/8 agonists are particularly effective against pancreatic cancer.^{30–32} This is likely a result of targeting and repolarizing the abundant suppressive myeloid populations inherent to the PDAC TME. We hypothesized that systemically administered TLR7/8 ligand R848, in combination with local SBRT, would generate not only local but also systemic antitumor immune responses by modulating the suppressive pancreatic TME and enhancing in situ vaccination of SBRT.

Here, we demonstrate that the combination of R848 and SBRT results in superior local tumor control and survival when compared with no treatment or monotherapy groups in two separate, clinically relevant PDAC tumor models. Significant changes to the cellular composition of the TME, including a skewing toward immunostimulation based on the cytokine/chemokine milieu, were observed in the combination treatment group. Importantly, systemic administration of R848 and local SBRT to the primary pancreatic tumor also elicited a distant antitumor immune response (ie, outside the field of radiation) against established hepatic metastases, and this response was dependent on CD8⁺ T cells. Mechanistic insight into this observation revealed the importance of systemic R848 in repolarizing the metastatic TME, whereas SBRT modified the T cell receptor (TCR) repertoire. Together, the combination therapy created a setting in which high-quality TCR clones were able to infiltrate into the now inflammatory TME of the metastases. Our results provide preclinical data suggesting the therapeutic use of TLR7/8 agonists in combination with SBRT to treat patients with locally advanced or metastatic PDAC.

METHODS

Cells and reagents

The murine PDAC KCKO and luciferase-expressing KCKO (KCKO-Luc) cell lines were a gift from Dr Pinku Mukherjee (University of North Carolina, Charlotte, North Carolina, USA, 2010). OVA-expressing KCKO (KCKO-OVA) and KP2 cell lines were generously provided by Dr David Denardo (Washington University of Medicine, St. Louis, Missouri, USA, 2016). Luciferase-expressing KP2 cells (KP2.1-Luc) were generated by transfecting the KP2 cells with luciferase-containing vectors. All cell lines were negative for *Mycoplasma* and cultured in RPMI1640 supplemented with 10% fetal bovine serum (FBS) and 1% penicillin/streptomycin. All the cell lines

used for experiments were within three passages of subsequent culture.

R848 (resiquimod) was purchased from Invivogen (cat# tlr1-r848-5). For *in vitro* experiments, 5 µg/mL of R848 were added in the complete culture medium. For *in vivo* experiments, 3 mg/kg were administered by retro-orbital injections (diluted in PBS, 100 µL per mouse) 1 day before, 1 day after, and 1 week after SBRT treatments (total of 3 times). For CD8⁺ T cell depletion, 200 µg of anti-CD8 (clone: 53–6.7) antibody or isotype rat immunoglobulin G (IgG) (diluted in phosphate buffered saline (PBS), 100 µL per mouse) were administered intraperitoneally every 3 days.

Murine orthotopic model and hepatic metastases model of pancreatic cancer

Six–eight-week-old female C57BL/6J mice were purchased from Jackson Laboratory and allowed to acclimate in the institutional animal facility. All animal studies have been approved by the University Committee on Animal Resources (UCAR) at the University of Rochester Medical Center (Rochester, NY). For the orthotopic model, mice were anesthetized with isoflurane and injected in the tail of the pancreas with 2×10^5 KCKO-Luc cells or 2.5×10^4 KP2.1-Luc cells in a 1:1 PBS to Matrigel suspension as described previously.²¹ Two small titanium clips were placed on either side of the tumor for identification at the time of SBRT. For the hepatic metastases model, mice that cured primary pancreatic tumors after SBRT plus R848 treatment were rechallenged with hemisplenic injection of 4×10^5 KP2.1-Luc cells in PBS to develop hepatic metastases as described previously.²¹ For the murine model with both orthotopic (2×10^5 KCKO cells or 2.5×10^4 KP2.1 cells) and hepatic metastases (4×10^5 KCKO-Luc cells or 4×10^5 KP2.1-Luc cells), mice were injected in the hemispleen with luciferase-expressing tumor cells and injected in the tail of the pancreas with tumor cells without luciferase.

SBRT treatment

Tumor-bearing mice were treated with SBRT as previously described.²¹ In brief, mice were anesthetized with isoflurane and transferred to a Small Animal Radiation Research Platform (XStrahl) equipped with a CT scanning device that is controlled by Muriplan software. A CT image of the mouse was taken to identify the pancreatic tumor based on two small metal fiducial clips placed on either side of the tumor at the time of injection. A dose of 6 Gy (X-ray) was delivered to the tumor using a 5-millimeter collimator for 4 consecutive days, with the beam angle precisely targeting the tumor to minimize normal tissue radiation exposure.

Flow cytometry

Mouse tumors were minced and digested with 30% collagenase (30 min, 37°C). Single-cell suspensions were generated by passing tumor fragments resuspended in 5% FBS through 40-micrometer cell strainer. Single-cell

suspensions were subsequently incubated with Fc receptor blocking solution followed by fluorophore-conjugated mouse antibodies (BD Biosciences or Biolegend). For cell surface staining, fluorescence-labeled antibodies, including anti-CD45, anti-CD3, anti-CD4, anti-CD8, anti-natural killer 1.1 (anti-NK1.1), anti-CD11b, anti-Ly6C, anti-Ly6G, anti-CD11c, anti-major histocompatibility complex class II (anti-MHCII), anti-CD80, anti-CD86, anti-programmed cell death protein 1 (anti-PD1), and anti-CTLA4, were added to samples for 30 min at 4°C in the dark. For further intracellular staining, cells were washed with PBS supplemented with 5% FBS, permeabilized with permeabilization buffer (BD Biosciences), and stained with fluorescence-labeled mouse antibodies, including anti-interferon gamma (IFN γ), anti-granzyme B (GzmB), antitumor necrosis factor alpha, and anti-FoxP3, for 30 min at 4°C in the dark. Stained cells were washed and resuspended in 5% FBS in PBS. Flow cytometry was performed on an LSRII, and data analyzed using FlowJo.

Immunohistochemical staining

The cleaved caspase-3, HMGB1, or calreticulin-positive cells were determined by immunohistochemical staining as described previously.²¹ Briefly, the frozen sections of tumor tissue from KCKO-Luc or KP2.1-Luc bearing mice were stained with primary antibodies, including cleaved caspase-3 (#9664S, Cell Signaling Technology), anti-HMGB1 antibody (ab18256, Abcam), or anti-calreticulin antibody (ab4109, Abcam), followed by horseradish peroxidase-labeled secondary antibody staining. 3,3'-Diaminobenzidine (DAB) was applied as substrate and hematoxylin as counterstaining. Positive cells were enumerated using a computerized Olympus DP80 imaging system. For cleaved caspase-3 or HMGB1 staining, 10 randomly selected fields ($\times 400$, magnification) of each tumor tissue section were enumerated, and the means were reported. The calreticulin expression in tumor tissue was examined and scored by a licensed pathologist (blinded): 0, no staining; 1, low intensity of staining, or $<25\%$ of tumor cells were positive; 2, medium level of intensity of staining, or $>25\%$ and $<50\%$ of tumor cells are positive; 3, the high-level intensity of staining, or $>50\%$ and $<75\%$ of tumor cells are positive; or 4, the maximum high-level intensity of staining, or $>75\%$ of tumor cells are positive.

Analysis of cytokines and chemokines by multiplexed magnetic Luminex assay

Tumor tissue samples were homogenized and digested with lysis buffer #11 (R&D Systems) containing protease inhibitors on ice for 1 hour. The samples were then centrifuged at 14,000 rpm for 20 min at 4°C, and supernatants were collected. Blood samples were centrifuged at 3000 rpm for 5 min at 4°C, and supernatants were collected as plasma. Cytokines and chemokines in tumor tissue or plasma were analyzed using a mouse premixed multianalyte kit according to manufacturer's instruction (USA R&D Systems). Samples with twofold dilution were run in a 96-well plate using the customized multiplex

cytokine/chemokine panels. A Bio-Rad BioPlex 200 analyzer was used to determine the mean fluorescence intensity (MFI) for 50 beads per analyte. The MFIs were compared with the standard curve using a five-parameter logistic regression analysis program.

Antigen presentation assay (B3Z T cell hybridoma activation)

Mice bearing KCKO-OVA in the pancreas were treated with SBRT (6 Gy on day 7, day 8, day 9, and day 10) and/or R848 (3 mg/kg, on day 6 and day 11). Mice were sacrificed on day 12 for the collection of tumor-draining lymph nodes (pancreaticoduodenal nodes) and the spleen. Cells were mechanically dissociated by passing through a 70-micrometer strainer, washed with RPMI1640, and incubated with B3Z T cell hybridoma to assess antigen presentation as previously described.²¹ Briefly, B3Z cells, which are OVA/K^b-specific cytotoxic T cell clone transfected with lacZ gene under the interleukin 2 (IL-2) promoter receptor, recognize the OVA₂₅₇₋₂₆₄ peptide (SIINFEKL) presented by H-2^b MHC and express lacZ on activation. Recognition of OVA peptide SIINFEKL by TCR leads to transcriptional activation of IL-2 promoter elements, resulting in the production of the enzyme β-galactosidase. Activated B3Z cells will turn blue on the addition of 5-bromo-4-chloro-3-indolyl-β-D-galactopyranoside (Thermo Fisher Scientific).

A total of 5×10^5 cells isolated from lymph node or spleen were incubated with 5×10^5 B3Z cells in 96-well flat-bottom plates in MAT/P medium (US patent 4.816.401) supplemented with 100 U/mL penicillin, 100 μg/mL streptomycin, and 5% fetal calf serum (FCS) for 18 hours at 37°C. Cells were washed with PBS and fixed with cold 2% formaldehyde with 0.2% glutaraldehyde for 10 min at 4°C. Cells were washed again with PBS and overlaid with 0.5 mg/mL 5-bromo-4-chloro-3-indolyl-β-D-galactopyranoside. The blue cells in each well were counted microscopically after 24 hours of incubation at 37°C.

Antigen-specific T cell detection

Mice orthotopic model or hepatic metastases model of pancreatic cancer was established with KCKO-OVA cells. For the orthotopic model, mice were injected with 2×10^5 KCKO-OVA cells in the pancreas tail and treated with SBRT on day 7, day 8, day 9, and day 10 and/or R848 on day 6 and day 11 after tumor implantation. For the orthotopic and hepatic models of pancreatic cancer, mice were injected with KCKO-OVA in the pancreas tail and liver (via hemisplenic injection) and treated with SBRT (tumor in the pancreas only) and retro-orbital R848 in the same manner as those of the orthotopic model. Treated mice were sacrificed on day 12 and H-2K^b (SIINFEKL) dextramer-binding CD8⁺ T cells in the tumor were determined by flow cytometry. Briefly, single-cell digests from tumor tissue were washed with PBS and stained with Aqua fluorescent reactive dye to identify the dead cells. Cells were then stained with H-2K^b (SIINFEKL) dextramer-PE (Immudex) at room temperature for 10 min, followed by staining of other surface markers (CD45-APC, CD3-FITC,

and CD8-PerCP-Cy5.5) for 20 min at 4°C. Stained cells were analyzed by flow cytometry within 2 hours. Aqua⁺Dextramer⁺CD45⁺CD3⁺CD8⁺ cells were determined as tumor antigen-specific T cells.

Antigen-presenting cells (APCs) activation in vitro with R848

CD11c⁺ DCs were generated from bone marrow (BM) of C57BL/6J mice as previously described.²¹ Briefly, BM cells were harvested from the femurs of mice, and 1×10^7 cells were cultured in 10 mL complete RPMI1640 containing mouse recombinant granulocyte macrophage-colony stimulating factor (GM-CSF) (50 ng/mL) and IL-4 (25 ng/mL) for 7 days, with fresh media containing GM-CSF and IL-4 added on day 4. R848 (5 μg/mL) was added into the culture media to activate DCs on day 8 and cultured for 24 hours. DCs were gated on CD11c and MHCII, CD80 and CD86 were analyzed as activation markers. For macrophage activation, R246.7 cells were cultured with R848 (5 μg/mL) for 24 hours, and expression of MHCII, CD80, and CD86 was analyzed.²¹

TCR repertoire analysis

Pooled single-cell suspensions (5 mice/group) from pancreatic tumor or liver metastatic tumor were prepared by enzymatic dissociation as previously described. Cells were stained with a panel of fluorophore-conjugated anti-mouse antibodies, including anti-CD45, anti-CD3, and anti-CD8. CD45⁺CD3⁺CD8⁺ T cells were then sorted on a FACSAria II (BD Biosciences). RNA extraction (RNeasy plus, Qiagen), TCR sequencing (TCR-seq) (MiSeq v3 and mouse TCR library), and analysis were performed by the University of Rochester Genomic Research Center. TCR-seq data analyses were run through MiXCR (MiLabs) using a pipeline for the analysis of enriched targeted TCR/IG libraries. The pipeline performed alignment of raw sequencing reads, assembly of aligned sequences into clonotypes, and output the resulting clonotypes into tab-delimited files. The list of final clones generated by MiXCR was further analyzed using VDJtools (MiLabs) or Immunarch. The TCR Diversity Index (chao1) was calculated from randomly downsampling of each sample to the least reads (from group 'liver mets=SBRT+R848') for 100 times. The Morisita's Index was used to assess the similarity of TCR repertoires between samples, taking into account the specific rearrangements and their respective frequencies and ranging from 0 (completely distinct TCR repertoire) to 1 (identical TCR repertoire).

Statistical analysis

Statistical analyses were performed with GraphPad Prism V.8 software. Unless indicated, data are expressed as mean ± SEM. For multiple group comparison studies, one-way ANOVA was used, followed by the Dunnett test for comparing experimental groups against the untreated group or monotherapy group as controls. For a single comparison between the two groups, the paired Student's t-tests were used. For survival comparison, log-rank

(Mantel-Cox) tests were used. A p value of <0.05 was considered to be significant.

RESULTS

R848 significantly enhanced antitumor efficacy of SBRT in murine orthotopic PDAC models

We investigated whether the TLR7/8 agonist R848 can improve the therapeutic efficacy of SBRT using established murine PDAC orthotopic models. The luciferase-expressing cell lines KCKO, derived from spontaneous PDAC tumors in p48-Cre/LSL-Kras^{G12D} mice, and the more aggressive KP2.1, derived from PDAC tumors in p48-Cre/LSL-Kras^{G12D}/p53^{fllox/+} mice, were orthotopically

injected into the tail of the pancreas. Tumor-bearing mice were divided into four experimental groups: (1) no treatment, (2) treated with a clinically relevant 6Gy×4 dose of SBRT, (3) intravenous R848, or (4) a combination of both therapies as shown in figure 1A. Tumor growth was monitored by a luciferase-detecting IVIS. SBRT or R848 monotherapies had minimal effects on tumor growth; however, the combination of SBRT and R848 significantly decreased tumor burden (figure 1B,C, KCKO, and figure 1E,F, KP2) and increased overall survival (figure 1D,G) in both tumor models. These data illustrate that the combinatorial approach resulted in approximately 50% of mice being cured of their tumor burden.

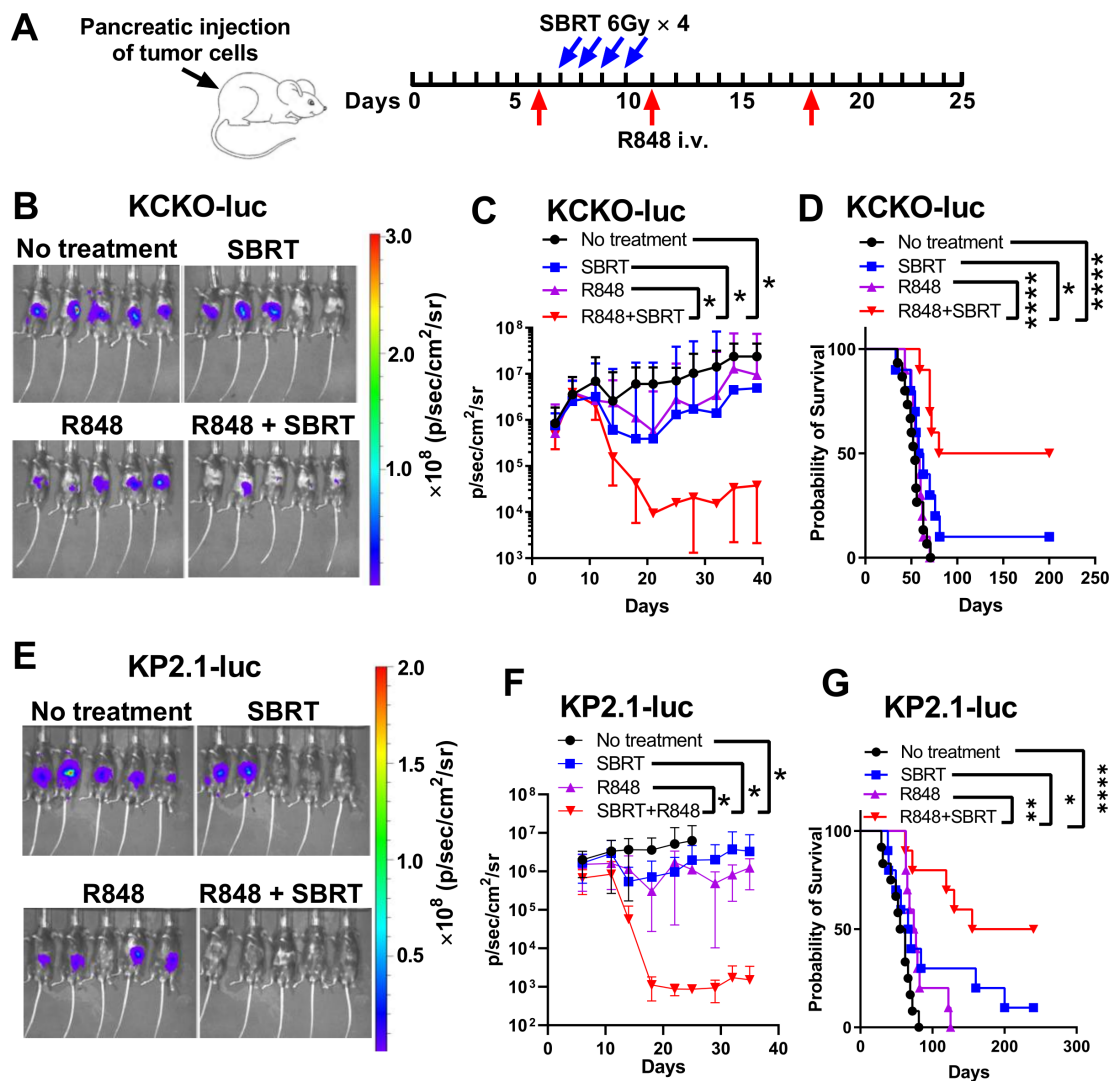


Figure 1 R848 significantly enhances the antitumor efficacy of SBRT in the murine orthotopic model of pancreatic cancer. (A) Schematic of the experimental design. C57BL/6J mice were injected with KCKO-Luc or KP2.1-Luc cells in the tail of pancreas and treated with SBRT and/or R848. Tumor growth was analyzed by IVIS twice a week. Representative IVIS images from day 19 after KCKO-Luc (B) or KP2.1-Luc (E) implantation. Tumor growth curve based on IVIS imaging, with (C) and (F) being KCKO-Luc and KP2.1-Luc, respectively. Data represent at least two independent experiments ($n=5-7$ mice/group). * $p<0.05$, SBRT+R848 compared with SBRT or R848 alone. Kaplan-Meier survival curves of mice bearing KCKO-Luc (D) or KP2.1-Luc (G) tumors. Data combined from two individual experiments. * $p<0.05$; ** $p<0.01$; **** $p<0.0001$. SBRT+R848 compared with no treatment group or monotherapy groups by log-rank (Mantel-Cox) test. IVIS, in vivo imaging system; i.v., intravenous; KCKO-Luc, luciferase-expressing KCKO; KP2.1-Luc, luciferase-expressing KP2 cells; $p/\text{sec}/\text{cm}^2/\text{sr}$, photons/second/ cm^2 /steradian; SBRT, stereotactic body radiation therapy.

Radiotherapy-induced immunogenic cell death is not augmented by R848

Previous work in our laboratory identified the induction of ICD/DAMPs as a key radiation-induced component that initiates an antitumor immune response following SBRT in KCKO pancreatic tumor model.²¹ We then investigated whether R848 therapy may augment ICD when used in combination with SBRT. Tumors from the four experimental groups (untreated, SBRT, R848, or SBRT/R848) were examined for evidence of cleaved caspase 3 (apoptotic cell death marker), or two DAMP markers, HMGB1 and calreticulin, by IHC. In both KP2.1 and KCKO models, SBRT alone could induce increased ICD and DAMP markers on both KP2.1 and KCKO

cells; however, R848 did not induce ICD/DAMPs alone or augment ICD/DAMPs in combination with SBRT (figure 2, KP2; online supplemental figure 1, KCKO). These results indicate that R848 is enhancing therapeutic efficacy by another mechanism besides directly inducing additional ICD/DAMPs in both orthotopic models.

The combination of SBRT and R848 modulates intratumor immune cell populations and cytokine/chemokine milieu

TLR7/8 is expressed on a variety of immune cells types, including DCs, monocytes, and macrophages, and may modulate the tumor immune microenvironment.^{23 25 27 33} To determine the impact of SBRT/R848 on the tumor immune microenvironment, we assessed multiple intratumoral

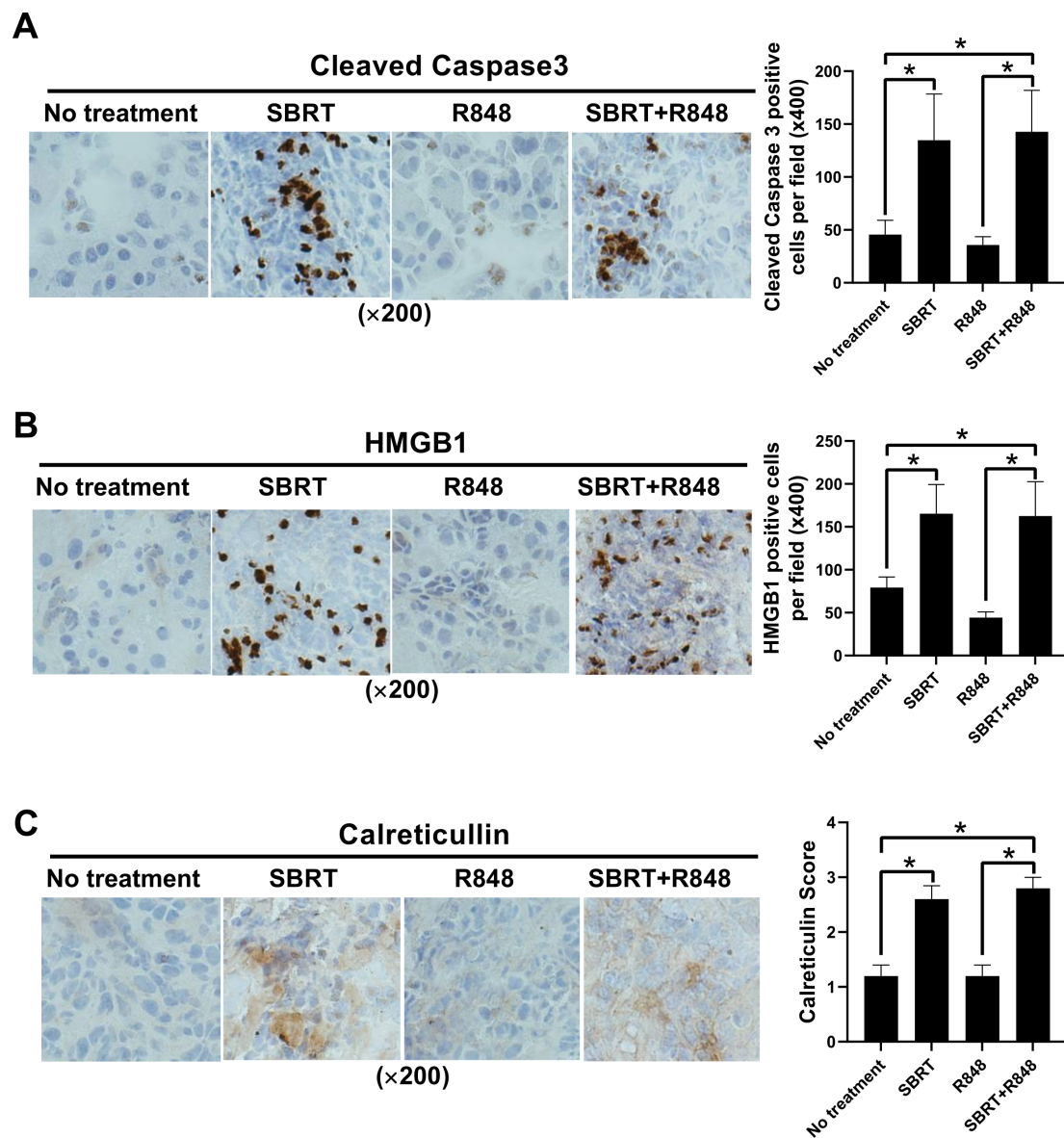


Figure 2 Treatment of SBRT, but not R848, induced tumor immunogenic cell death in the orthotopic model of murine pancreatic cancer. Mice bearing KP2.1-Luc orthotopic pancreatic tumors were treated with SBRT and/or R848, and ICD was determined by immunohistochemistry (IHC) staining of cleaved caspase 3 (A), HMGB1 (B), and calreticullin (C). Results are expressed as mean±SEM from five mice/group and analyzed by one-way analysis of variance (ANOVA) with Dunnett posttest. * $p < 0.05$, compared with no treatment group or monotherapy groups. ICD, immunogenic cell death; KP2.1-Luc, luciferase-expressing KP2 cells; SBRT, stereotactic body radiation therapy.

immune populations by flow cytometry at day 12, which represents a time point following the completion of SBRT and administration of 2 doses of R848. CD8⁺ T cells were significantly increased in the combined treatment group (figure 3A and online supplemental figure 2A–E). Notably, only CD8⁺ T cells in the R848+SBRT group exhibited heightened IFN γ and GzmB staining. Other regulatory markers (CTLA-4 and PD-1) were similar between the different groups. These data suggest that both the percentage and effector status of CD8⁺ T cells are elevated by combined therapy. Additionally, CD4⁺ T cells were reduced when tumors were treated with SBRT, but importantly, the addition of R848 further decreased the potentially immunosuppressive population of CD4⁺/FOXP3⁺ T cells in the combined treatment group (figure 3B and online supplemental figure 2F–H). Consistent with the previous finding that NK cells are involved in TLR7/8 induced immune response,^{33–35} the percentage of NK cells was significantly augmented by R848 when combined with SBRT. These data highlight the importance of the combinatorial approach in promoting an antitumor phenotype in the effector immune cell populations.

The combination of R848 and SBRT did not alter the percentages of myeloid immune subsets, including tumor-associated macrophages (TAMs), monocytic and granulocytic MDSCs and DCs (figure 3C–E, respectively, and online supplemental figure 2I–N). Given that TLR7/8 ligands are known to promote antigen-presenting cell (APC) activation and maturation,²⁵ we found that R848 significantly upregulates surface expression of MHCII, CD80, and CD86 on DCs and macrophages after 24 hours in vitro (online supplemental figure 3). Consistently, in the tumor, R848 monotherapy and especially the combination therapy increased co-stimulatory molecules, CD80 and CD86, in both TAMs (figure 3C) and DCs (figure 3E) suggesting a skewing toward a mature, immunostimulatory phenotype.

We also examined the change of intratumoral cytokines and chemokines after SBRT and/or R848 treatment in KCKO tumor homogenate using Luminex technology. The combined treatment group demonstrated a comprehensive increase of factors commonly associated with antitumor potential (eg, IFN γ , GzmB, CXCL10, etc), and decrease of protumor factors [eg, IL-4, IL-6, IL-10, CXCL12, vascular endothelial growth factor (VEGF), etc] (figure 3F and online supplemental figure 4). Collectively, our data from figure 3 suggest that combination treatment results in a conversion of the TME from immunosuppressive to one that promotes antitumor potential.

The combination of SBRT and R848 promotes DC antigen presentation and subsequent generation of local effector CD8⁺ T cells

Combined therapy results in superior local tumor control (figure 1) and significantly modulates a multitude of immunological factors (figure 3) that may promote local antitumor immunity. Additionally, we established that DCs exhibited an enhanced maturation

status following combined therapy (figure 3E). Therefore, to further investigate the mechanism of action, we used a KCKO-OVA model (figure 4A) to assess antigen presentation using an established B3Z hybridoma assay as described in the materials and methods. Although both monotherapies induced activated B3Z cells (as a readout for antigen presentation), combined therapy induced the greatest antigen presentation in the tumor draining lymph node but also in the non-draining lymph node and spleen as well (figure 4B). This level of antigen presentation resulted in an increase of tumor-specific intratumoral CD8⁺ T cells as determined by H-2K^b/SIIN-FEKL dextramer staining (figure 4C) and quantified in (figure 4D). Importantly, the tumor-reactive CD8⁺ T cells were highest in the combined therapy group and deemed essential as antibody depletion of CD8⁺ T cells significantly abrogated treatment efficacy (figure 4E,F). These data demonstrate the generation of CD8⁺ T cells was critical for the observed local antitumor therapeutic effect.

Combination therapy exerts a systemic antitumor response against liver metastases

The majority of patients with PDAC present with metastatic disease, where the liver is the most common site for dissemination. Effective therapies against this aggressive malignancy will likely need to induce potent systemic antitumor responses. Data presented in figure 4B demonstrate that APCs were capable of presenting tumor antigen in sites distal to the tumor (eg, nondraining lymph node and spleen) suggesting that combination therapy may promote the generation of local but also systemic antitumor immunity. To test this, R848+SBRT treated mice cured of primary KP2 pancreatic tumors for at least 50 days were rechallenged with a hemisplenic administration of KP2-Luc. figure 5A,B demonstrate that combined therapy results in long-lasting, systemic immunologic memory capable of rejecting a hepatic challenge. We employed a murine model bearing both orthotopic KCKO or KP2 (unlabeled) primary pancreatic tumors and metastatic KCKO-Luc or KP2-Luc (labeled) tumors in the liver to examine if the combined treatment approach is effective in controlling established liver metastases (figure 5C). It is important to note that only the primary pancreatic tumor is targeted with SBRT, whereas R848 therapy is given systemically. Combined therapy dramatically slowed hepatic tumor growth and promoted survival in both the KCKO (figure 5D,E) and KP2 (figure 5F,G) metastatic models, suggesting an abscopal effect. These data demonstrated that the combination treatment with R848 and SBRT could amplify systemic antitumor immune responses, resulting in enhanced metastatic control.

R848 reshapes the metastatic TME

Combined therapy results in superior hepatic tumor control compared with the other experimental groups including R848 monotherapy (figure 5). We performed endpoint experiments to evaluate whether R848+SBRT elicited a unique change in the hepatic foci that

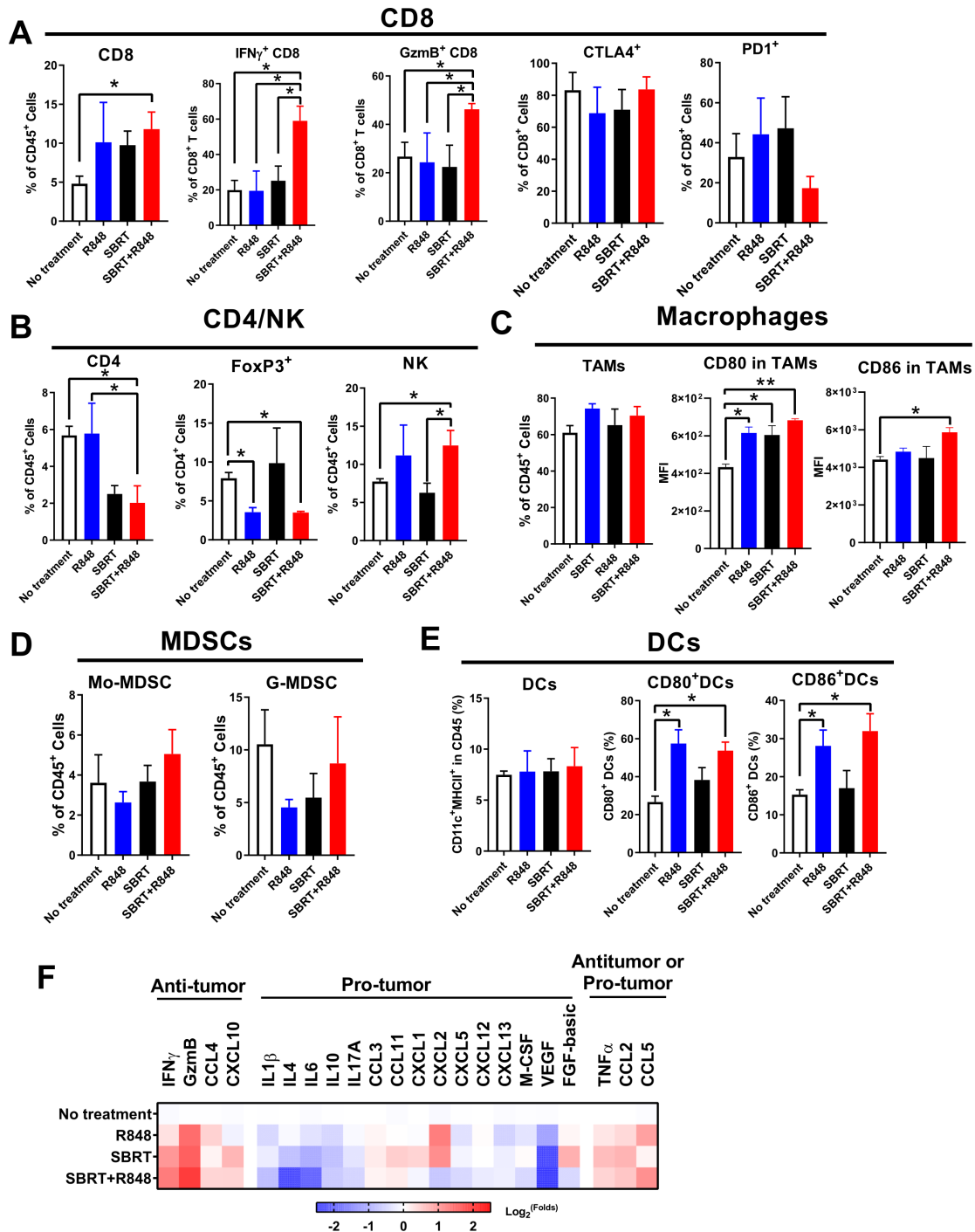


Figure 3 SBRT combined with R848 enhances antitumor immune response in the orthotopic model of murine pancreatic cancer. Mice bearing KCKO-Luc orthotopic pancreatic tumors were treated with SBRT on day 7, day 8, day 9 and day 10, and/or R848 on day 6 and day 11. Mice were sacrificed on day 12, tumor-infiltrating immune cells were determined by flow cytometry, and tumor cytokines and chemokines were determined by multiplex Luminex assay. (A) Tumor-infiltrating CD8⁺ T cells, CD8⁺IFN γ ⁺, CD8⁺GzmB⁺, CD8⁺CTLA4⁺, and CD8⁺programmed cell death protein 1 (PD1)⁺ cells were analyzed. (B) Tumor-infiltrating CD4⁺ T cells, Tregs, and natural killer (NK) cells were analyzed. (C) TAMs and their expression of CD80 and CD86 were analyzed. (D) MDSCs, including Mo-MDSC and G-MDSC populations, were shown. (E) Tumor-infiltrating DCs, CD80⁺DCs, and CD86⁺DCs were analyzed. Results are expressed as mean \pm SEM from five mice/group and analyzed by one-way analysis of variance (ANOVA) with Dunnett posttest. Significance is indicated by * p <0.05 and ** p <0.01, compared with no treatment group or monotherapy. (F) Fold changes of cytokines and chemokines in the tumor following treatment of SBRT/R848. Levels of cytokines and chemokines of tumors from mice of no treatment group were set as 1, and data were fold changes as compared with no treatment group. DCs, dendritic cells; IFN γ , interferon gamma; G-MDSC, granulocytic myeloid derived suppressor cell; GzmB, granzyme B; KCKO-Luc, luciferase-expressing KCKO; MDSCs, myeloid derived suppressor cells; Mo-MDSC, monocytic myeloid derived suppressor cell; SBRT, stereotactic body radiation therapy; TAMs, tumor-associated macrophages; Tregs, regulatory T cells.

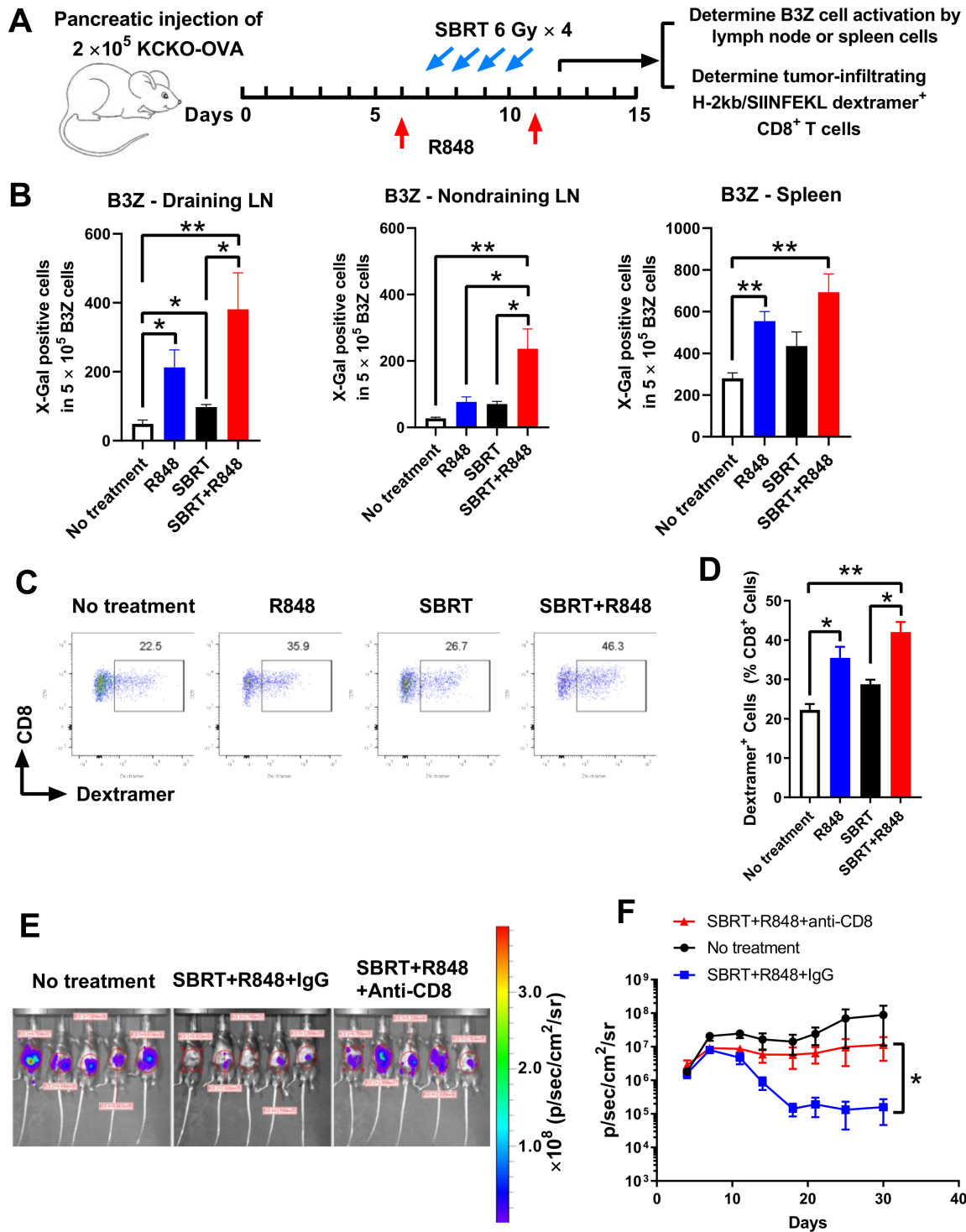


Figure 4 CD8⁺ T cells are vital for the antitumor effect of SBRT/R848 in the orthotopic model of murine pancreatic cancer. (A) Schematic of experimental design. KCKO-OVA pancreatic tumor bearing mice were treated with SBRT and/or R848 and mice were sacrificed on day 12, antigen presentation was detected by B3Z T-cell activation, and antigen-specific CD8⁺ T cells were determined by flow cytometry. (B) Enhanced antigen presentation following SBRT/R848 treatment. Antigen presentation was detected by B3Z T-cell hybridoma activation assay after coculture with cells from draining or non-draining lymph nodes or spleen. Results are expressed as mean \pm SEM from five mice/group and analyzed by one-way analysis of variance (ANOVA) with Dunnett posttest. * p <0.05 and ** p <0.01, compared with no treatment group or monotherapy group. Representative of flow cytometry plots (C) and quantitative analysis (D) for H2K^b/SIINFEKL⁺Dextramer⁺CD8⁺ T cells. (D) Data are represented as mean \pm SE (n =5 for each group). * p <0.05 and ** p <0.01, compared with no treatment group or monotherapy. Representative of IVIS image on day 19 (E) and tumor growth curve (F) based on IVIS after treated with SBRT+R848 with/without CD8⁺ T cell depletion. Data are represented as mean \pm SE (n =5 for each group). * p <0.05; SBRT+R848+CD8 depletion group compared with SBRT+R848+IgG group. IVIS, in vivo imaging system; KCKO-OVA, OVA-expressing KCKO; SBRT, stereotactic body radiation therapy.

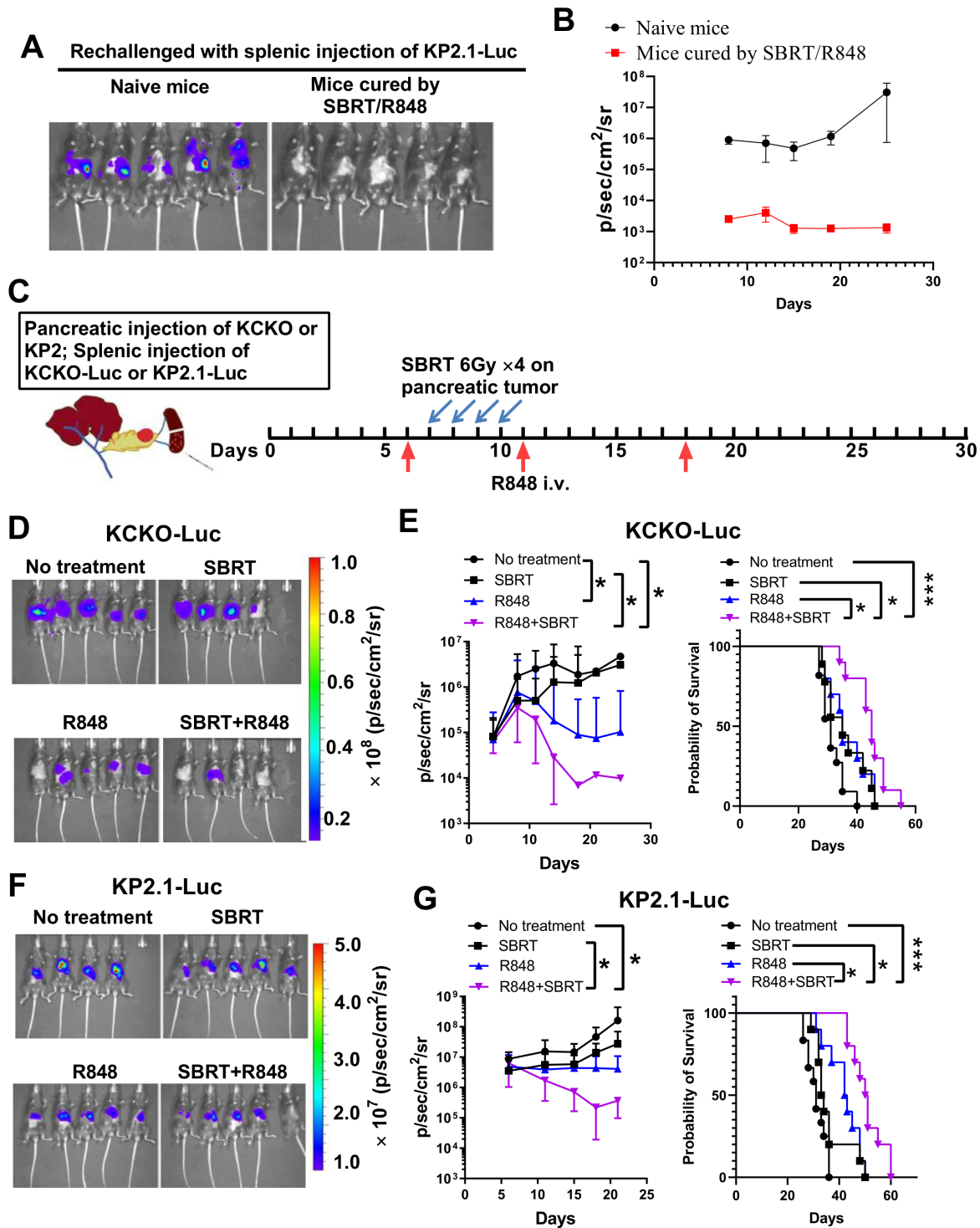


Figure 5 Systemic R848 and local SBRT treatment exert synergistic antitumor effects on liver metastasis of pancreatic cancer. (A) and (B) Naïve mice or mice that cured of KP2.1-Luc tumors after SBRT/R848 treatment were given KP2.1-Luc via splenic injection. Representative IVIS imaging of hepatic tumor metastasis on day 19 post-tumor injection and tumor growth curve based on IVIS were shown. (B) Results are expressed as mean±SEM from five mice/group. (C) Schematic of orthotopic pancreatic cancer and hepatic metastasis establishment, and treatment with SBRT and R848. Representative IVIS imaging of hepatic tumor metastasis on day 14 following KCKO-Luc (D) or KP2.1-Luc (F) tumor injection. The growth of liver metastases of KCKO-Luc (E, left panel) or KP2.1-Luc (G, left panel) was analyzed by IVIS imaging. Tumor burden was observed at random either at the pancreas or liver, and in some case, both sites exhibited tumor growth. Data are expressed as mean±SEM from 5 mice/group, representing 2 individual experiments. Kaplan-Meier survival curves of mice bearing KCKO and KCKO-Luc (E, right panel) or KP2 and KP2.1-Luc (G, right panel) tumors are combined from 2 individual experiments. * $p < 0.05$, ** $p < 0.01$, and *** $p < 0.001$, compared with no treatment group or monotherapy by one-way ANOVA with Dunnett posttest for growth curve or by log-rank (Mantel-Cox) test for survival curve. IVIS, in vivo imaging system; KCKO-Luc, luciferase-expressing KCKO; KP2.1-Luc, luciferase-expressing KP2 cells; p/sec/cm²/sr, photons/second/cm²/steradian; SBRT, stereotactic body radiation therapy.

contributed to metastatic tumor control. Primary and hepatic KCKO tumors were generated as described in figure 5C, where only the primary tumor was treated with SBRT, whereas R848 was given systemically. Liver metastases were taken for flow cytometric and Luminex analysis on day 12. Interestingly, R848 induced small but significant changes in CD8⁺ T cell, CD4⁺ FoxP3 T regulatory cell, and CD11b⁺ myeloid cell frequencies regardless of whether it was used as a monotherapy or combined with SBRT (online supplemental figure 5). The comprehensive Luminex panel complemented the flow cytometric data as R848 monotherapy and R848+SBRT have remarkably similar expression levels of cytokines and chemokines with a shift toward immunostimulation (online supplemental figure 6). These data highlight that systemic administration of R848 is sufficient to modulate the metastatic TME toward immune activation regardless of whether it is combined with SBRT.

Combination therapy generates a unique repertoire of CD8⁺ T cells that are pivotal for the antitumor effect on liver metastases

Analysis of the metastatic immune microenvironment did not reveal significant differences between R848 monotherapy and combined therapy (online supplemental figures 5 and 6) even though the combined treatment group demonstrated superior tumor control. To further address this observation, we shifted our focus to CD8⁺ T cells as we hypothesized that combined therapy may improve the quality of this effector immune population. Using the KCKO dual primary and metastatic model described in figure 5C, we determined that CD8⁺ T cells were essential in mediating the metastatic antitumor effect of combined therapy, as antibody depletion of CD8⁺ T cells abrogated treatment efficacy in the R848+SBRT group when compared with IgG controls (figure 6A,B). Furthermore, combined treatment in the KCKO-OVA model (figure 6C) resulted in the highest frequency of tumor-specific H-2K^b/SIINFEKL Dextramer⁺CD8⁺ T cells in metastatic foci; however, similar increases in this cell population were also observed with R848 monotherapy (figure 6D,E).

To ascertain if combined therapy may alter the TCR repertoire of CD8⁺ T cells, we established both primary and metastatic tumors as in figure 7A, and FACS sorted CD8⁺ T cells from both the primary pancreatic tumor and hepatic foci to perform TCR-Seq. Results demonstrated fewer clonotypes and a trend toward increased clonality after SBRT monotherapy; however, similar frequency distributions and numbers of unique clonotypes were observed between R848 and SBRT+R848 groups (figure 7B and online supplemental figure 7A). Furthermore, although both R848 and SBRT+R848 groups were found to be more clonotypically diverse relative to no treatment and SBRT alone, no differences were observed between R848 and SBRT+R848 groups (figure 7C and online supplemental figure 7B). In liver metastases, all four groups also demonstrated similar numbers of unique

clonotypes, repertoire frequency distributions, and clonal diversity (figure 7D,E and online supplemental figure 7C,D). However, a more comprehensive analysis of TCR repertoires revealed marked conservation of clonotypes between combo-treated primary and metastatic tumors, as indicated by an increased Morisita's overlap index relative to untreated and monotherapy groups (figure 7F and online supplemental figure 7E). These findings were corroborated by top T cell clonotype tracking analysis, which identifies overlapping TCR clones between two different anatomical sites (eg, primary and metastatic tumors). Importantly, the combination group exhibited the most overlap of TCR clones between the primary and metastatic sites (5 out of the top 10 clones—overlapping clones highlighted in purple) when compared with the other experimental groups (figure 7G and online supplemental figure 7F). These findings collectively suggest that R848+SBRT treatment results in the expansion of high-quality T cell clonotypes that are capable of infiltrating both primary and metastatic lesions, indicative of systemic antitumor immunity.

DISCUSSION

In this study, we have demonstrated that systemic administration of the TLR7/8 agonist, R848, greatly augmented the SBRT-induced antitumor response in mouse orthotopic and metastatic PDAC models. Mechanistically, SBRT induces ICD locally at the site of irradiation releasing tumor antigens, while R848 amplifies the vaccination effect by activating APCs and modulating the immunosuppressive TME in PDAC, leading to enhanced antitumor effects. Importantly, this combination therapy also generates a durable systemic antitumor response, providing a promising strategy for the treatment of advanced/metastatic PDAC.

Substantial evidence suggests that SBRT is more immunogenic compared with conventional radiation, making it a good backbone treatment to be combined with immunotherapies.^{36,37} SBRT likely induces tumor cells to undergo ICD, resulting in the cell surface expression and/or release of DAMPs and tumor antigens. This in turn leads to the activation of APCs and induction of tumor antigen-specific T cell responses.²² We have previously demonstrated that SBRT induces ICD in various mouse pancreatic cancer models.²¹ Here, we observed increased ICD in the tumor after SBRT treatment in murine orthotopic KCKO and KP2 models. Radiotherapy has been shown to convert an immunologically 'cold' tumor into an immunologically 'hot' lesion.³⁸ We observed that SBRT alone induced DC and macrophage activation, and elevated levels of intratumoral IFN γ , GzmB, CCL2, CXCL2, and CXCL10. However, SBRT alone was insufficient to significantly control tumor growth or prolong survival in vivo, which may be due to the immunosuppressive nature of the pancreatic TME, which ultimately limits the recruitment and efficacy of antitumor immune responses. Therefore, combining radiotherapy with

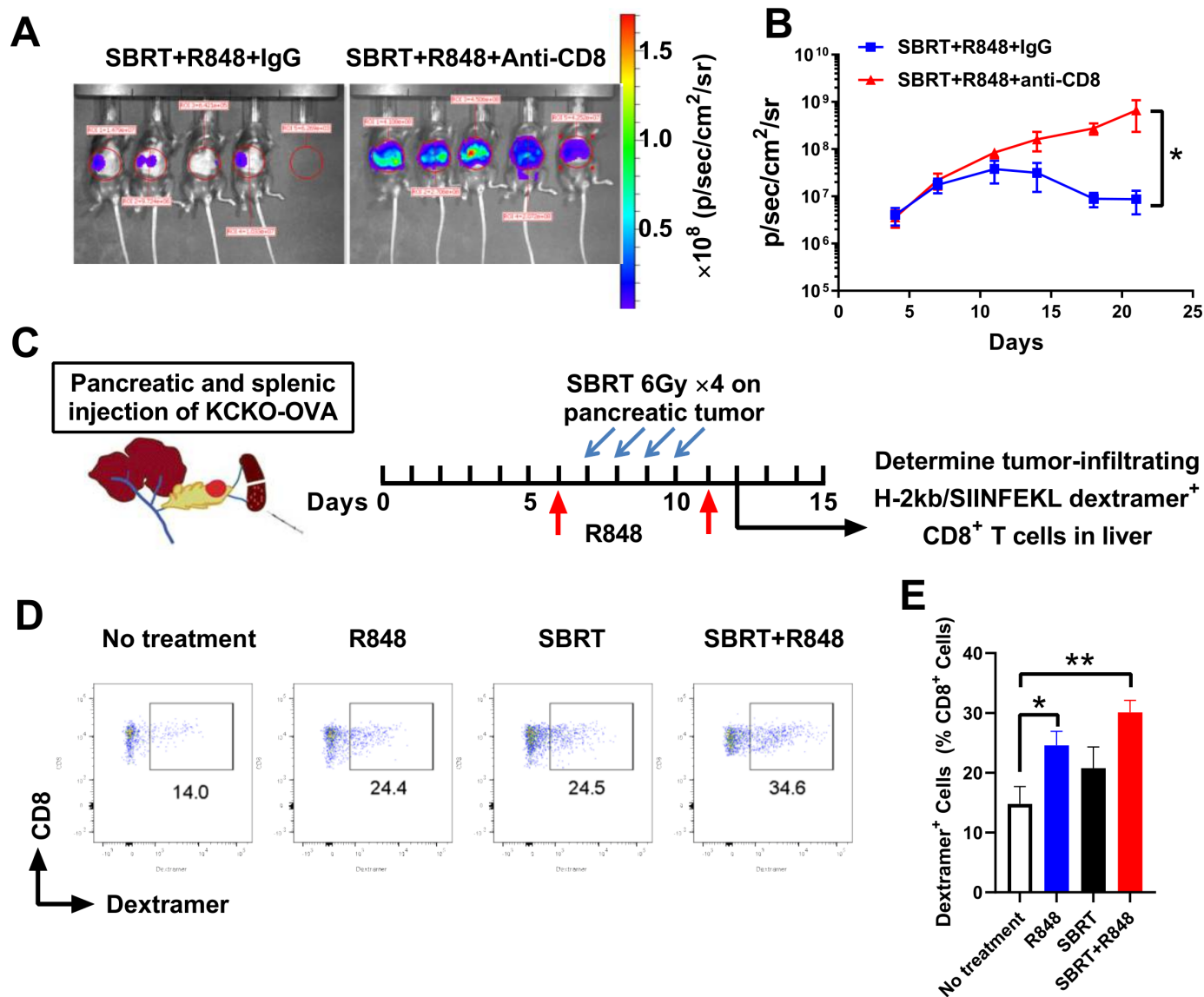


Figure 6 CD8⁺ T cells are essential for the antitumor efficacy of SBRT and R848 in liver metastasis. (A) and (B) Mice bearing orthotopic pancreatic tumors and hepatic metastases were treated with SBRT and R848, with or without CD8⁺ T cell depletion. Shown in (A) is representative IVIS imaging of hepatic tumor metastases on day 14 following KCKO-Luc injection. The growth of liver metastases was analyzed by IVIS imaging as in (B). Data are expressed as mean \pm SEM from 4 mice/group to 5 mice/group. * $p < 0.05$; SBRT+R848+CD8 depletion group compared with SBRT+R848+IgG group. (C) Schematic of experimental design. KCKO-OVA pancreatic and hepatic tumor bearing mice were treated with SBRT and/or R848. Mice were sacrificed on day 12 and antigen-specific CD8⁺ T cells from liver metastasis were determined by flow cytometry. (D) and (E) Representative of flow cytometry plots (D) and quantitative analysis (E) for H2K^b/SIINFEKL⁺Dextramer⁺CD8⁺ T cells after treatment with or without SBRT and/or R848. Data are expressed as mean \pm SEM from 5 mice/group. * $p < 0.05$ and ** $p < 0.01$, compared with no treatment group. IVIS, in vivo imaging system; KCKO-Luc, luciferase-expressing KCKO; KP2.1-Luc, luciferase-expressing KP2 cells; KCKO-OVA, OVA-expressing KCKO; p/sec/cm²/sr, photons/second/cm²/steradian; SBRT, stereotactic body radiation therapy.

exogenous adjuvants such as TLR agonists that further stimulate and reprogram the TME may overcome this immunosuppression, facilitating the induction of effective antitumor immune responses.

There are conflicting results regarding the use of TLR7/8 agonists as a treatment for cancer. One early study demonstrated that TLR7 agonists may promote carcinogenesis in the spontaneous KC pancreatic models³⁹; however, recent evidence supports the antitumor effect of TLR7/8 agonists in pancreatic cancer. For example,

one study demonstrated that higher TLR7 expression is correlated with a better prognosis in human PDAC,⁴⁰ and this was further supported by another study showing that the lack of TLR1/3/7/9 expressions in PDAC was indicative of a poor prognosis.⁴¹ In preclinical models, the TLR7/8 agonist R848 was shown to remodel tumor and host responses to promote overall survival in an orthotopic murine model of pancreatic cancer.³² Another study using a non-clinically relevant Pan02 PDAC model (derived from carcinogen 3-methylcholanthrene) has

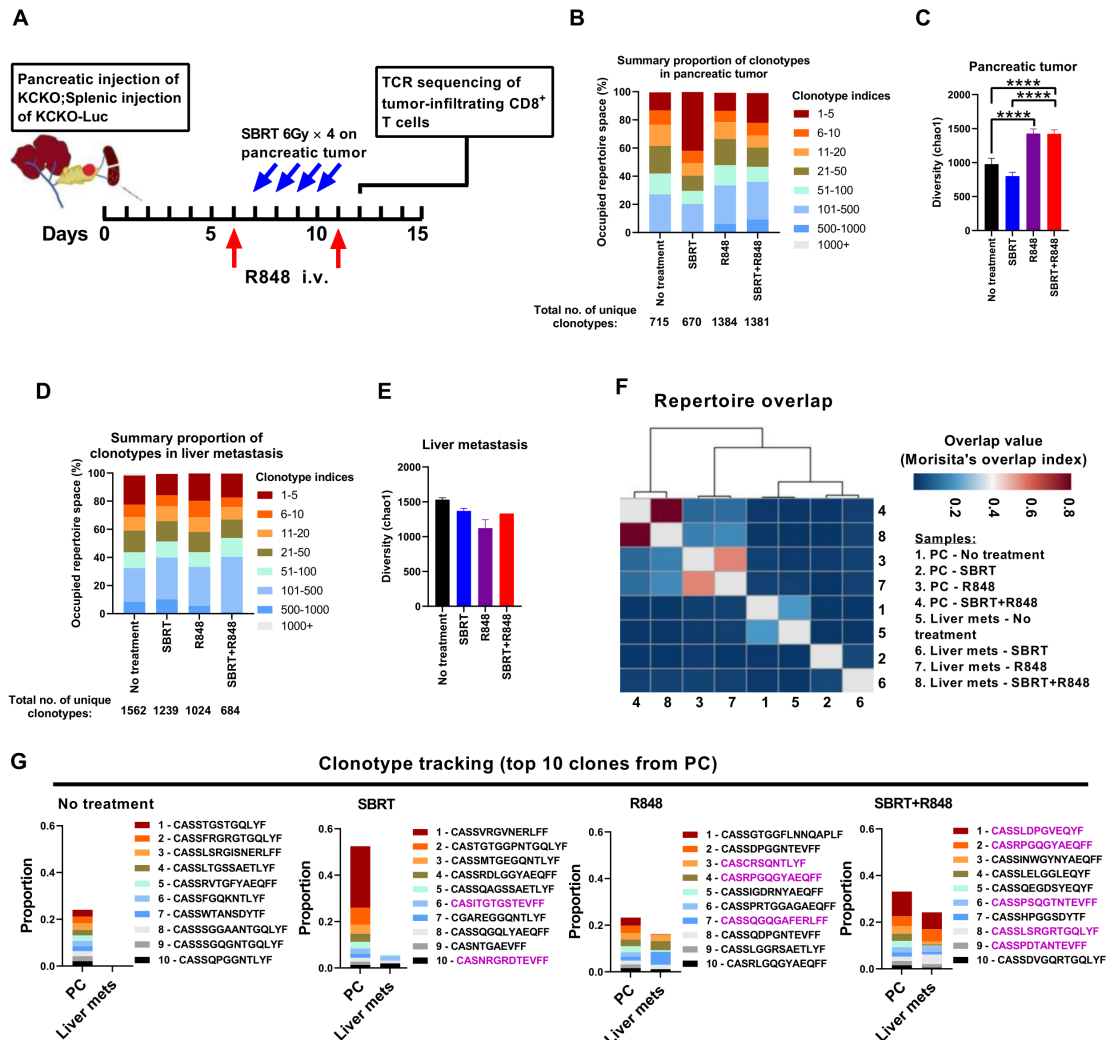


Figure 7 Combination of SBRT and R848 increases overlapping TCR clonotypes between the primary pancreatic tumor and liver metastasis. Mice bearing KCKO tumors in pancreas and liver were treated with SBRT only at primary tumor site (pancreas), R848 systemically, or combination of SBRT/R848 as illustrated in (A). On day 12 after tumor inoculation, mice were sacrificed and TCR sequence of tumor infiltrating CD8⁺ T cells sorted from pooled tumor samples (5 mice/group) were analyzed. Summary proportion of clonotypes with specific indices were analyzed in pancreatic tumor (B) and liver metastases (D) showing SBRT or SBRT/R848 increased frequency of top 5 TCR β clone types in pancreatic tumor. The diversity (chao 1) of TCR β clonotypes in pancreatic tumor (C) and liver metastases (E) from different treatment groups was calculated from randomly downsampling of each sample to the least reads (liver mets—SBRT+R848 group), showing R848 or SBRT/R848 increased diversity of TCR β clonotypes in pancreatic tumor but not in liver metastasis. (F) TCR β repertoire overlap (Morisita's overlap index) was analyzed showing that combination of SBRT and R848 resulted in highest TCR β overlap between pancreatic tumor and liver metastasis. (G) Clonotype tracking of 10 top TCR β clonotypes in pancreatic tumor infiltrating CD8⁺ T cells was analyzed in liver metastasis showing highest similarity of respective clonotype frequency between pancreatic tumor and liver metastasis following SBRT/R848 treatment. i.v., intravenous; KCKO-Luc, luciferase-expressing KCKO; KP2.1-Luc, luciferase-expressing KP2 cells; KCKO-OVA, OVA-expressing KCKO; SBRT, stereotactic body radiation therapy; TCR, T cell receptor; PC, pancreatic cancer.

shown that combination of TLR7/8 ligand 3M-011 with radiotherapy significantly reduced both primary and distal tumors in mesenteric lymph nodes of the small intestine.⁴² These data suggested that R848 may be a good candidate to combine with SBRT to enhance PDAC therapeutic efficacy. These conflicting results prompted us to specifically develop a clinically relevant preclinical PDAC model in order to improve our understanding of how this TLR agonist may actually behave in patients with PDAC. Our model includes orthotopic injection of two different cell lines harboring PDAC-specific driver

mutations (KRAS in KCKO and KRAS and p53 in KP2) that more closely resembles human PDAC, a clinically relevant SBRT schedule, including the use of CT-targeting fiducial markers, and a hepatic metastatic model that recapitulate the most common type of PDAC dissemination observed in patients. Using our model, a number of differences were observed. First, in contrast to a prior study,²⁵ we found R848 did not induce ICD in the tumor in vivo, nor did it increase SBRT-induced ICD, suggesting R848 has no direct effect on promoting tumor cell death or DAMP release. Second, our data suggest that R848 is

quite ineffective as a monotherapy. This differs with a recent study that demonstrated R848 monotherapy could effectively extend survival in an orthotopic pancreatic mouse model.³² The observed discrepancy may be due to the models used and/or the different therapeutic schedules where R848 (3 mg/kg) was given intravenous weekly for a total of 3 weeks in our study compared with 10 µg intraperitoneal injection (i.p.) daily for long-term in the other study. This suggests that the duration of R848 treatment may impact its efficacy, and a long-term maintenance treatment may be useful. In agreement with other reports,⁴³ we also demonstrated that R848 monotherapy was able to repolarize the TME that resulted in an increase of DC and macrophage activation and antigen presentation. However, R848 alone could not significantly increase CD8⁺ T cell and NK cell infiltration, echoing its inability to elicit durable T cell responses in other animal models.⁴³ These results, coupled with the limited effectiveness of SBRT alone, strongly suggest for a combinatorial approach that harnesses the positive antitumor attributes of both R848 and SBRT together.

Our results clearly demonstrate that systemic R848 greatly potentiates SBRT-induced local tumor growth inhibition and prolongs survival in different orthotopic PDAC models. This is particularly important as 30% of patients with PDAC die from localized disease.² This enhanced antitumor effect is mainly due to significant immune cell frequency changes, including increased CD8⁺ T cells (especially the IFNγ⁺CD8⁺ T cells and GzmB⁺CD8⁺ T cells), NK cell infiltration, and decreased regulatory T cell (Treg) infiltration. This treatment also altered the local cytokine/chemokine profile by decreasing intratumoral suppressive cytokines (IL-4, IL-6, and IL-10) while increasing antitumor cytokines (IFNγ and GzmB) and proinflammatory cytokines (CCL2, CCL5, and CXCL10). It is likely that the repolarization of the TME contributes to enhanced functionality of CD8⁺ T cells as illustrated by increases in both antigen-specific SIINFEKL⁺ CD8⁺ T cells and IFNγ⁺GzmB⁺CD8⁺ T cells following combined treatment. Importantly, SBRT alone increased TCR clonality; however, the addition of R848 promoted a more clonally diverse subset that coincided with superior local tumor control. We hypothesize this is due to the merger of (1) R848 diversifying the TCR repertoire and (2) SBRT generating unique TCR clones that recognize neoantigens released by irradiated tumor cells. Overall, SBRT and R848 cooperatively reprogram the local TME from immunosuppressive to immunostimulatory, and this promotes a potent adaptive antitumor immune response.

Systemic antitumor responses following local therapy are a rare event clinically.⁴⁴ This is likely due to a myriad of factors, including low immunogenic tumors with an immunosuppressive TME at both the local and metastatic sites. Our results demonstrate that R848 greatly improves systemic antitumor immunity when combined with local SBRT in two different PDAC models. This growth inhibition is accompanied by significant changes of immune cell infiltration into metastatic (nontargeted) liver sites, including increased infiltration of

antigen specific and overall CD8⁺ T cells, decreased infiltration of Tregs and MDSCs, as well as a reduction of IL-10 levels and increased GzmB and CCL5 expression. Interestingly, these differences were also seen in liver metastases from the R848 only group but did not result in effective metastatic control. These differences highlight the importance combined therapy has on the generation of CD8⁺ T cells as critical effectors in mediating this response. First, CD8⁺ T cell depletion significantly reduced metastatic protection. Second, TCR repertoire analysis suggested that R848 was required to prime/repolarize the distal hepatic TME to allow for infiltration of immunodominant clonotypes generated by SBRT. This is emphasized by our clonotype tracking data showing that 5 out of the 10 most abundant TCR clones are located in both the local and metastatic sites (compared with only 2 out of 10 in the SBRT only treated group). However, whether the CD8 T cell clonal change in primary and metastatic tumors is tumor-specific still remains to be studied. In general, our data suggest that systemic R848 therapy is required to modulate the TME in both the primary and metastatic pancreatic cancer sites to facilitate entry of SBRT-primed CD8⁺ T cells. This study provides a proof of principle for the translation of combined SBRT/R848 therapy for the treatment of both locally advanced and/or metastatic PDAC.

Author affiliations

¹Department of Surgery, University of Rochester Medical Center, Rochester, New York, USA

²Center for Tumor Immunology Research, University of Rochester Medical Center, Rochester, New York, USA

³Wilmot Cancer Institute, University of Rochester Medical Center, Rochester, New York, USA

⁴Department of Microbiology and Immunology, University of Rochester Medical Center, Rochester, New York, USA

⁵Department of Pediatrics, University of Rochester Medical Center, Rochester, New York, USA

Twitter Joseph D Murphy @josephdmurphy

Contributors Conception and design: JY, DCL and SAG. Development of methodology: JY, CJJ, EML, DCL and SAG. Acquisition of data: JY, BNM, JDM, JG-L, TPU, BJH, and TGV. Analysis and interpretation of data: JY, SSQ, BNM, and SAG. Writing, review, and/or revision of the manuscript: JY, EML, BAB, DCL, TPU, and SAG. Administrative, technical, or material support: BJH and CJJ. Guarantors: JY and SAG. Study supervision: DCL and SAG.

Funding This work was supported by grants from the NIH (R01CA230277 to SAG; R01CA236390 to SAG and Elizabeth Repasky; and R01CA262580 to SAG and DCL). We additionally thank Eric Hernady of the Small Animal Radiation Research Core and Dr John Ashton of University of Rochester Medical Center Genomics Research Core.

Competing interests None declared.

Patient consent for publication Not applicable.

Ethics approval Not applicable.

Provenance and peer review Not commissioned; externally peer reviewed.

Data availability statement All data relevant to the study are included in the article or uploaded as supplementary information.

Supplemental material This content has been supplied by the author(s). It has not been vetted by BMJ Publishing Group Limited (BMJ) and may not have been peer-reviewed. Any opinions or recommendations discussed are solely those of the author(s) and are not endorsed by BMJ. BMJ disclaims all liability and responsibility arising from any reliance placed on the content. Where the content includes any translated material, BMJ does not warrant the accuracy and reliability of the translations (including but not limited to local regulations, clinical guidelines,

terminology, drug names and drug dosages), and is not responsible for any error and/or omissions arising from translation and adaptation or otherwise.

Open access This is an open access article distributed in accordance with the Creative Commons Attribution Non Commercial (CC BY-NC 4.0) license, which permits others to distribute, remix, adapt, build upon this work non-commercially, and license their derivative works on different terms, provided the original work is properly cited, appropriate credit is given, any changes made indicated, and the use is non-commercial. See <http://creativecommons.org/licenses/by-nc/4.0/>.

ORCID iD

Jian Ye <http://orcid.org/0000-0002-6955-9262>

REFERENCES

- Siegel RL, Miller KD, Jemal A. Cancer statistics, 2020. *CA Cancer J Clin* 2020;70:7–30.
- Rawla P, Sunkara T, Gaduputi V. Epidemiology of pancreatic cancer: global trends, etiology and risk factors. *World J Oncol* 2019;10:10–27.
- The guidelines of the National comprehensive cancer network (NCCN). Available: <https://www.nccn.org/patients/guidelines/content/PDF/pancreatic-patient.pdf>
- De Bari B, Porta L, Mazzola R, et al. Hypofractionated radiotherapy in pancreatic cancer: lessons from the past in the era of stereotactic body radiation therapy. *Crit Rev Oncol Hematol* 2016;103:49–61.
- Petrelli F, Comito T, Ghidini A, et al. Stereotactic body radiation therapy for locally advanced pancreatic cancer: a systematic review and pooled analysis of 19 trials. *Int J Radiat Oncol Biol Phys* 2017;97:313–22.
- Trakul N, Koong AC, Chang DT. Stereotactic body radiotherapy in the treatment of pancreatic cancer. *Semin Radiat Oncol* 2014;24:140–7.
- Chuong MD, Springett GM, Freilich JM, et al. Stereotactic body radiation therapy for locally advanced and borderline resectable pancreatic cancer is effective and well tolerated. *Int J Radiat Oncol Biol Phys* 2013;86:516–22.
- Shaib WL, Hawk N, Cassidy RJ, et al. A phase 1 study of stereotactic body radiation therapy dose escalation for borderline resectable pancreatic cancer after modified FOLFIRINOX (NCT01446458). *Int J Radiat Oncol Biol Phys* 2016;96:296–303.
- Bayne LJ, Beatty GL, Jhala N, et al. Tumor-derived granulocyte-macrophage colony-stimulating factor regulates myeloid inflammation and T cell immunity in pancreatic cancer. *Cancer Cell* 2012;21:822–35.
- Clark CE, Beatty GL, Vonderheide RH. Immunosurveillance of pancreatic adenocarcinoma: insights from genetically engineered mouse models of cancer. *Cancer Lett* 2009;279:1–7.
- Clark CE, Hingorani SR, Mick R, et al. Dynamics of the immune reaction to pancreatic cancer from inception to invasion. *Cancer Res* 2007;67:9518–27.
- Panni RZ, Sanford DE, Belt BA, et al. Tumor-induced STAT3 activation in monocytic myeloid-derived suppressor cells enhances stemness and mesenchymal properties in human pancreatic cancer. *Cancer Immunol Immunother* 2014;63:513–28.
- Porembka MR, Mitchem JB, Belt BA, et al. Pancreatic adenocarcinoma induces bone marrow mobilization of myeloid-derived suppressor cells which promote primary tumor growth. *Cancer Immunol Immunother* 2012;61:1373–85.
- Stromnes IM, Brockenbrough JS, Izeradjene K, et al. Targeted depletion of an MDSC subset unmasks pancreatic ductal adenocarcinoma to adaptive immunity. *Gut* 2014;63:1769–81.
- Stromnes IM, Greenberg PD, Hingorani SR. Molecular pathways: myeloid complicity in cancer. *Clin Cancer Res* 2014;20:5157–70.
- Nywenning TM, Belt BA, Cullinan DR, et al. Targeting both tumour-associated CXCR2⁺ neutrophils and CCR2⁺ macrophages disrupts myeloid recruitment and improves chemotherapeutic responses in pancreatic ductal adenocarcinoma. *Gut* 2018;67:1112–23.
- Nywenning TM, Wang-Gillam A, Sanford DE, et al. Targeting tumour-associated macrophages with CCR2 inhibition in combination with FOLFIRINOX in patients with borderline resectable and locally advanced pancreatic cancer: a single-centre, open-label, dose-finding, non-randomised, phase 1B trial. *Lancet Oncol* 2016;17:651–62.
- Bernard B, Rajamanickam V, Dubay C, et al. Transcriptional and immunohistological assessment of immune infiltration in pancreatic cancer. *PLoS One* 2020;15:e0238380.
- Mills BN, Qiu H, Drage MG, et al. Modulation of the human pancreatic ductal adenocarcinoma immune microenvironment by stereotactic body radiotherapy. *Clin Cancer Res* 2022;28:150–62.
- Galluzzi L, Vitale I, Warren S, et al. Consensus guidelines for the definition, detection and interpretation of immunogenic cell death. *J Immunother Cancer* 2020;8:e000337.
- Ye J, Mills BN, Zhao T, et al. Assessing the magnitude of immunogenic cell death following chemotherapy and irradiation reveals a new strategy to treat pancreatic cancer. *Cancer Immunol Res* 2020;8:94–107.
- Golden EB, Apetoh L. Radiotherapy and immunogenic cell death. *Semin Radiat Oncol* 2015;25:11–17.
- Baird JR, Monjazebe AM, Shah O, et al. Stimulating innate immunity to enhance radiation therapy-induced tumor control. *Int J Radiat Oncol Biol Phys* 2017;99:362–73.
- Blasius AL, Beutler B. Intracellular toll-like receptors. *Immunity* 2010;32:305–15.
- Smits ELJM, Ponsaerts P, Berneman ZN, et al. The use of TLR7 and TLR8 ligands for the enhancement of cancer immunotherapy. *Oncologist* 2008;13:859–75.
- Tyring S. Imiquimod applied topically: a novel immune response modifier. *Skin Therapy Lett* 2001;6:1–4.
- Vasilakos JP, Tomai MA. The use of Toll-like receptor 7/8 agonists as vaccine adjuvants. *Expert Rev Vaccines* 2013;12:809–19.
- Dovedi SJ, Melis MHM, Wilkinson RW, et al. Systemic delivery of a TLR7 agonist in combination with radiation primes durable antitumor immune responses in mouse models of lymphoma. *Blood* 2013;121:251–9.
- Adlard AL, Dovedi SJ, Telfer BA, et al. A novel systemically administered Toll-like receptor 7 agonist potentiates the effect of ionizing radiation in murine solid tumor models. *Int J Cancer* 2014;135:820–9.
- Shojaei H, Oberg H-H, Juricke M, et al. Toll-like receptors 3 and 7 agonists enhance tumor cell lysis by human gammadelta T cells. *Cancer Res* 2009;69:8710–7.
- Zou B-B, Wang F, Li L, et al. Activation of Toll-like receptor 7 inhibits the proliferation and migration, and induces the apoptosis of pancreatic cancer cells. *Mol Med Rep* 2015;12:6079–85.
- Michaelis KA, Norgard MA, Zhu X, et al. The TLR7/8 agonist R848 remodels tumor and host responses to promote survival in pancreatic cancer. *Nat Commun* 2019;10:4682.
- Pradere J-P, Dapito DH, Schwabe RF. The yin and yang of Toll-like receptors in cancer. *Oncogene* 2014;33:3485–95.
- Dumitru CD, Antonyamsy MA, Gorski KS, et al. NK1.1+ cells mediate the antitumor effects of a dual Toll-like receptor 7/8 agonist in the disseminated B16-F10 melanoma model. *Cancer Immunol Immunother* 2009;58:575–87.
- Mullins SR, Vasilakos JP, Deschler K, et al. Intratumoral immunotherapy with TLR7/8 agonist MEDI9197 modulates the tumor microenvironment leading to enhanced activity when combined with other immunotherapies. *J Immunother Cancer* 2019;7:244.
- Rodriguez-Ruiz ME, Vitale I, Harrington KJ, et al. Immunological impact of cell death signaling driven by radiation on the tumor microenvironment. *Nat Immunol* 2020;21:120–34.
- Popp I, Grosu AL, Niedermann G, et al. Immune modulation by hypofractionated stereotactic radiation therapy: therapeutic implications. *Radiother Oncol* 2016;120:185–94.
- Portella L, Scala S. Ionizing radiation effects on the tumor microenvironment. *Semin Oncol* 2019;46:254–60.
- Ochi A, Graffeo CS, Zambirinis CP, et al. Toll-like receptor 7 regulates pancreatic carcinogenesis in mice and humans. *J Clin Invest* 2012;122:4118–29.
- Narayanan JSS, Ray P, Hayashi T, et al. Irreversible electroporation combined with checkpoint blockade and TLR7 stimulation induces antitumor immunity in a murine pancreatic cancer model. *Cancer Immunol Res* 2019;7:1714–26.
- Lanki M, Seppänen H, Mustonen H, et al. Toll-like receptor 1 predicts favorable prognosis in pancreatic cancer. *PLoS One* 2019;14:e0219245.
- Schölch S, Rauber C, Tietz A, et al. Radiotherapy combined with TLR7/8 activation induces strong immune responses against gastrointestinal tumors. *Oncotarget* 2015;6:4663–76.
- Frega G, Wu Q, Le Naour J, et al. Trial Watch: experimental TLR7/TLR8 agonists for oncological indications. *Oncoimmunology* 2020;9:1796002.
- Demaria S, Formenti SC. The abscopal effect 67 years later: from a side story to center stage. *Br J Radiol* 2020;93:20200042.